

1 Manuscript category: **Original scientific paper**

2

3

Decay of the melt stream during dispersion in granulation devices

4

5 Vsevolod I. Sklabinskiy¹, Artem E. Artyukhov^{1,*}, Mykola P. Kononenko¹, Jan Krmela²

6

¹*Sumy State University, Sumy, Ukraine*

7

²*Alexander Dubcek University of Trencin, Trencin, Slovak Republic*

8

9

10

11

12

13

14

15

16

17

18

19 ***Corresponding author:** Artem E. Artyukhov, Sumy State University; E-mail:

20 a.artyukhov@pohnp.sumdu.edu.ua;

21

22

23

24
25
26
27
28
29
30
31
32
33
34
35
36
37
38
39
40
41
42
43
44
45

ABSTRACT

The aim of the article is a theoretical description and experimental study of the melt jet expiration process from a perforated shell. Mathematical modeling of hydrodynamic flows was carried out based on the points of classical fluid and gas mechanics and technical hydromechanics. Mathematical model equations were solved by using computer mathematics of Maple and wxMaxima. Reliability of the obtained experimental results is based on the application of time-tested in practice methods. Hydrodynamic properties of the liquid jet outflow were obtained. The presented mathematical model allows calculation of radial component of the jet outflow velocity, as well as determination of the influences of physical and chemical properties of the liquid and the outflow hole diameter on the jet length and flow velocity along the axis to its disintegration into separated drops. The developed mathematical model extended with the theoretical description of the melt dispersion process from rotating perforated shells allowed us to improve design of the granulator to stabilize hydrodynamic parameters of the melt movement. Consideration of hydrodynamic parameters of the fluid jet flowing out of the holes of the perforated membrane provides improvement of the construction of nitrogen fertilizers melt dispersant, affect to the parameters of the process of jet decay into drops, its size and monodispersity. Basket tests of the granulator was confirmed the theoretical research and provided a basis for modernization of the equipment construction.

Keywords: jet decay, vibration granulator, hydrodynamic of flows movement, melt dispersion process, rotating perforated shell

46

1. INTRODUCTION

47 Liquid dispersion processes forming micro- or macro drops are used in power generation,
48 medicine, chemical industry, agriculture and other spheres of human activity. Efficiency of these
49 technological processes and equipment is largely determined by the quality of liquid dispersion,
50 which usually involves obtaining monodisperse drops [1].

51 This fully applies to the production of the commodity form of nitrogen fertilizers, which is
52 carried out in two main ways [2]:

53 - granulation starting from the liquid phase by dispersion on the surface of suspended particles
54 in a fluidized bed that can be variously configured (technologies of Casale S.A., Switzerland; Kahl
55 Group, Germany; Stamicarbon, Netherlands; Toyo Engineering Corporation, Japan;
56 Thyssenkrupp Fertilizer Technology GmbH, Germany, etc.) [3-8], including vortex granulation [9,
57 10];

58 - granulation starting from the liquid phase by dispersion into drops followed by crystallization
59 of the solute by dewatering and cooling (prilling) (devices of Norsk Hydro, Norway; Didier
60 Engineering GmbH, Germany; Imperial Chemical Industries, UK; Kaltenbach-Thuring S.A.,
61 France et al.) [11].

62 In these methods, among others, devices with different forms of a perforated shell, generally
63 being axially symmetrical can be used for dispersion of the nitrogen fertilizer melt.

64 Devices for melt dispersion can be classified by the form of the working part (*i.e.* perforated
65 shell) and by the presence of internal devices in the perforated shell. Additionally, these devices
66 differ in the nature of force acting on the melt and can be static, swirl (tangential introduction of
67 the melt into a perforated shell or to the turbine for the melt spin), and dynamic (rotating) [12].

68 In recent years, preference is mainly given to conical or cylindrical rotating devices and devices
69 with the cup-shaped shell. This is due to simplicity of operation and high uniformity of resulting
70 liquid drops and commodity granules in comparison to analogue devices.

71 For example, ammonium nitrate granulators (dispersers), which are currently in operation,
72 provide manufacturing of products with following granulometric composition in terms of mass
73 fraction: 0.5 - 1.5 % of granules < 1.0 mm in size, 90 – 98 % of granules in the size range 2.0 - 4.0
74 mm, where granules in the size range 2.0 - 2.5 mm comprise 42 - 71% and granules in the size
75 range 2.0 - 3.0 mm comprise 85 - 95% [13, 14]. Dispersion of melts producing more than 2 % of
76 dust-forming particles of less than 1.0 mm and over 3.5 mm in size, which can be also
77 destructed making dust, leads to dust formation of nitrogenous fertilizers in air in the tower.

78 In existing equipment calculation of hydrodynamic characteristics of the liquid jet that is
79 dispersed is often not performed, resulting in lower uniformity of the obtained drops [15].
80 Hydrodynamic parameters of the liquid jet issuing from a single hole or holes of the perforated
81 shell, and design features of devices for fluid dispersion influence the process of jet decay into
82 drops.

83 The problem of creating the adequate model of jet decay into drops at the opening in a thin wall
84 is highly relevant for dispersion improvement in granulation devices in the mineral fertilizers
85 production. By controlling the jet decay process, we can optimize the performance of dispersant
86 and create favorable conditions to produce a product with a high degree of monodispersity.

87 The aim of the article is a theoretical description and experimental study of the melt jet outflow
88 process from a perforated shell (basket).

89

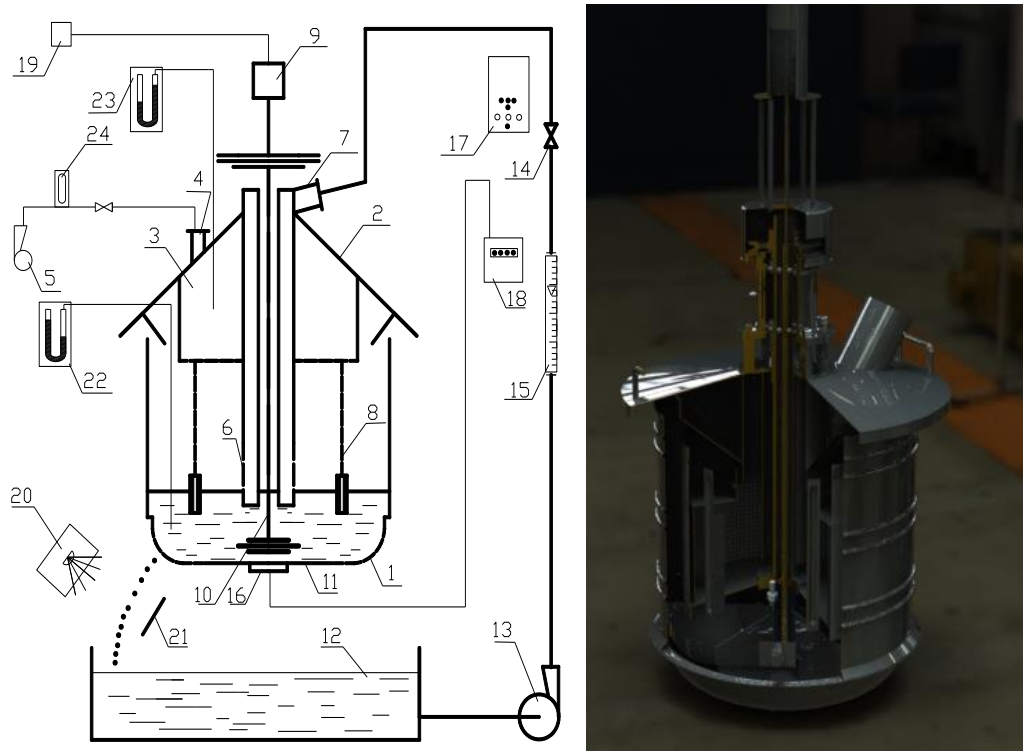
90 2. DESCRIPTION OF THE OBJECT AND METHODS OF RESEARCH

91 Mathematical modeling of hydrodynamic flows was carried out based on the postulates of
92 classical fluid and gas mechanics and technical hydromechanics [16, 17]. Solving equations of
93 mathematical models was carried out by using the Maple software (Maplesoft, Canada) [18]
94 and the open-source computer algebra system wxMaxima [19, 20]. These systems have proven
95 to provide reliable and efficient symbolic and numerical algorithms for a wide range of
96 mathematical problems, including a well-known library of numerical algorithms NAG (Numerical
97 Algorithms Group, UK). Adequacy of calculated dependences for the process that was
98 investigated, is validated by the comparison of calculated data with known and experimentally
99 obtained results.

100 2.1 Experimental vibrating granulator

101 A vibrating granulator (manufacturer – Sumy State University, Processes and Equipment of
102 Chemical and Petroleum-Refineries Department, Ukraine; granulator diameter is 560 mm,
103 granulator height is 590 mm) is the main unit of the experimental unit (Fig. 1), which consists of
104 a variable perforated membrane 1 with holes to discharge the fluid, housing 2 with a
105 distributive drive 3 and a pipe 4 for introducing air from the fan 5. The housing 2 is also supplied
106 with a fixed liquid distributor 6 with a pipe 7 and a filter element 8.
107 At the top of the fluid atomizer, a mechanical, electrical or electromagnetic vibrator 9 is
108 installed, which is connected by a rod 10 with the resonator 11 in the form of an elastic disc or
109 plate.
110 When the granulator is working, liquid that goes through the pipe 7 and the distributor 6 to the
111 bottom part of the granulator flows out of the holes of the perforated membrane.

112 Simultaneously, air at a given pressure is supplied by the fan 5 through the pipe 4 into the cavity
113 of the granulator.



114

115

a b



116

117

c

118 **Fig. 1. Experimental installation of the vibrating granulator. a) A schematic presentation of the**
119 **granulator (design features of elements which are not described – see [21]): 1- perforated**
120 **membrane (diameters of holes are 1.0 mm, 1.1 mm, 1.2 mm, 1,3mm, 1,4 mm, number of**
121 **holes is 1800-2300, bottom shape is toroidal, length is 650 mm, diameter is 560 mm), 2 –**
122 **housing (height is 590 mm, diameter is 560 mm), 3 – distributive drive, 4 – pipe (diameter is**

123 45 mm), 5 – fan, 6 – liquid distributor, 7 – pipe (diameter is 100 mm), 8 - filter element (metal
124 grid), 9 – vibrator (MFR OTY 77 actuator, range of output frequency 120-1200 is Hz), 10 – rod,
125 11 - resonator, 12 - buffer bunker, 13 – circulation pump (model Calpeda NC3 25-50/180), 14 –
126 valve, 15 – rotameter (model Raifil RF FM 10), 16 - oscillations sensor, 17 – oscillograph
127 (model C1-65A), 18 – digital frequency meter (model VC3165), 19 – electronic controller, 20,
128 21 – elements of stroboscope, 22, 23 – manometers (model MT-2Y), 24 – controller (model
129 Euroaqua SKD-1); b) 3D model of vibrating granulator; c) 3D model and photo of experimental
130 installation

131 The installation is equipped with a buffer bunker 12 for liquid with a circulation pump 13. Valve 14
132 and rotameter 15 are used to regulate and measure the liquid flowrate . The oscillations sensor 16
133 is connected with an oscillograph 17 to observe fluctuations while the digital frequency meter 18 is
134 used to measure the oscillation frequency. When the electrodynamic or electromagnetic vibrator is
135 used, regulation of oscillations is carried out by the electronic controller 19. A stroboscope (20 and
136 21) is installed for visual observation of the process of liquid dispersion into drops. Measurements
137 of the liquid pressure in holes and air at the free surface of the liquid are carried out by
138 manometers 22 and 23, respectively. The controller 24 is aimed to regulate the air pressure in the
139 granulator.

140 Next, the electronic oscillator 19 is switched on and the electrodynamic vibrator 9 started
141 resulting in vibration of the resonator at a certain frequency, which is fixed for the testimony of
142 digital frequency meter 18, which is connected to the vibration sensor 16 (measurer of
143 frequency) of the granulator basket. Air is supplied into the granulator volume by turning the
144 fan 5 on, then when the interstitial position is changed, the given pressure is installed based on
145 manometer data. The process of jets dispersion into drops is simultaneously monitored by using
146 a stroboscope 20. When formation of monodisperse drops (without satellite droplets) is

147 observed, measurements are recorded at the manometer 22 , which corresponds to the total
148 liquid pressure in the leakage holes, and at the digital frequency meter 18 showing the vibration
149 frequency (upper limit). These liquid and air parameters are changing by changing the vibration
150 frequency with electronic generator 19 by the lower limit of granulator stable operation range.
151 Ranges of stable operation are determined for different liquid leakage velocities from holes in
152 the basket, which can be achieved by changing the granulator performance under constant air
153 pressure or by changing the air pressure by using the pressure regulator at the constant
154 granulator performance. When operating the vibration granulator at different liquid leakage
155 velocities, the fluid flow rate is measured by a graduated cylinder.

156 Physical modeling is based on methods of the similarity theory. The geometric similarity is
157 maintained by equality of appropriate constants and invariants [22].

158 The special frequency generator is designed to generate vibration on the radiator of rotating
159 vibrational melting granulator by feeding electric signals of a special shape on the MFR OTY 77
160 actuator (system operation description - in accordance with [23]).

161 Main parameters and characteristics:

- 162 • frequency range of reproducible oscillations, Hz – 200 – 1000
- 163 • rated load, W – 50 – 100
- 164 • limits of the permissible relative basic error, setting of the oscillation frequency, % – 0.5
- 165 • voltage of the mains supply of the generator, V – 220±10
- 166 • frequency of the mains, Hz – 60
- 167 • active resistance of the moving coil, Ohm – 8
- 168 • established trouble-free operating time, h – 1000 (with a confidence probability 0,95)

169 Operating conditions:

- 170 • ambient temperature – -10 – + 70 ° C
- 171 • relative humidity – 50 – 80% at a temperature of +25 °C

172 • atmospheric pressure – 86 – 106.7 kPa

173 The special frequency generator consists of:

174 • Generator of electrical signals of a special form

175 • Actuator MFR OTY 77

176 The generator of electrical signals of a special form consists of:

177 • Block of digital synthesis of frequency

178 • The amplifier

179 • Power supply unit

180 Specifications of the electrical signal generator:

181 • frequency range – 200 – 1000 Hz

182 • the minimum frequency setting step is 0.01Hz

183 • output power – 60W

184 • load resistance – 3.7 Ohm

185 • harmonic coefficient at the frequency of 500 Hz – 0.1%

186 • load inductance – 7.3 mH

187 The digital synthesis unit performs direct digital frequency synthesis (DDS – Direct Digital
188 Synthesizer) and is implemented on a microprocessor. Due to this, the generator has a high
189 frequency stability and a small step of its tuning. The unit allows you to store 10 preset
190 frequencies in the non-volatile memory. Each of which can be easily changed during operation.
191 Indication of the generated frequency is carried out on the liquid crystal display.

192 The amplifier provides the necessary amplification of signals from the generator to feed them
193 into a low-resistance load. The amplifier is implemented on an integrated microcircuit. The
194 output stage is made on field-effect transistors. This ensures a high efficiency amplifier. The
195 amplifier has a built-in protection system against overload, overheating and "soft start" system.

196 To power the whole device a power supply made by the classical transformer scheme is used.
197 Two bipolar rectifiers supply a +/- 12V – the circuit for digital synthesis of frequency, and +/-
198 24V – amplifier.

199 Actuator MFR OTY 77

200 Electromagnetic vibrator consists of control block and vibro-converter. Control block is used for
201 delivery of a signal of set frequency and amplitude to vibro-converter. A signal received from
202 the control block, is transferred to the vibro-converter where under influence of magnetic field
203 a reorientation of crystal lattice of the core alloy material occurs. As a result the core changes its
204 length. The radiator of granulator's vibrations is joined to the bottom part of the core. Cooling
205 of vibro-converter is provided by cooling air expulsion. The vibro-system has an input and
206 output signal 4-20 mA what will allow to automatically control the frequency of vibration
207 depending on the change of the fusion level in granulator. Control block of the vibro-system is
208 fixed on CPU.

209

210 2.2 Processing of the experimental results

211 Velocity, V , of the liquid leaking from the granulator holes is calculated as:

$$212 \quad V = \phi \cdot \sqrt{2 \cdot g \cdot H}. \quad (1)$$

213 where ϕ is the discharge coefficient and set to 0.96-0.98 [24].

214 According to experimental data of upper f_1 and lower f_2 limits of the frequency, which provides

215 a monodisperse liquid jet decay, the maximum and minimum lengths of the wave are

216 calculated:

$$217 \quad \lambda_{\max} = V/f_1; \lambda_{\min} = V/f_2, \quad (2)$$

218 The melt flowrate, G_s , through the granulator hole is calculated from the measured leaked melt

219 volume, G_τ and time, τ :

$$220 \quad G_s = G_\tau / \tau. \quad (3)$$

221 Diameter of drops, formed by the decay of liquid jets at the average vibration frequency of the

222 granulator, f_{avi} , is determined from the material balance according to the equation:

223
$$d_{dr} = 3 \sqrt[3]{\frac{6 \cdot G_s}{\pi \cdot f_{avi}}}.$$
 (4)

224 The absolute difference of drop diameters and a relative deviation of drop diameters from the
 225 average drop diameter at the granulator maximum and minimum productivity are calculated as
 226 follows:

227
$$\Delta d_{dr}^{ab} = d_{dr}^{max} - d_{dr}^{min}.$$
 (5)

228
$$\Delta d_{dr}^{rel} = \frac{2(d_{dr}^{max} - d_{dr}^{min})}{d_{dr}^{max} + d_{dr}^{min}}.$$
 (6)

229 To define the optimal number of experiments and the highest accuracy degree and reliability of
 230 the obtained results, as well as for the processing of these results, methods of mathematical
 231 statistics were used [25].

232 Two types of measurement errors - random and systematic, may occur during the experiment
 233 conducting [26].

234 A random error reduces the accuracy of experiment results. An analysis of this type of error is
 235 possible by using the root-mean-square deviation σ , calculated by the following equation:

236
$$\sigma = \sqrt{\frac{\sum_{i=1}^n (\bar{x} - x_i)^2}{n-1}},$$
 (7)

237 where \bar{x} is the arithmetic mean value; x is the single parameter value; n is the number of
 238 measurements.

239 The maximum possible error of a single measurement, Δ , was determined by the three sigma
 240 rule:

241
$$\Delta = 3\sigma.$$
 (8)

242 The bilateral confidence interval of the arithmetic mean value ε was determined by the
243 following function [26], provided that this parameter is located in the confidence interval with
244 the probability not less than 95%:

$$245 \quad \varepsilon = t \frac{\sigma}{\sqrt{n}}, \quad (9)$$

246 where t is the Student's criterion [27].

247 The root-mean-square error of indirect measurements is calculated as:

$$248 \quad \sigma_y = \sqrt{\sum_{i=1}^n \left(\frac{\partial y}{\partial x} \cdot \Delta \cdot x_i \right)^2}, \quad (10)$$

249 where $y=f(x_1, x_2, \dots, x_n)$.

250 The accuracy of the obtained regression equations is determined by the least-squares method
251 [28].

252 The systematic measurement error had an identical effect on all parameters that were
253 controlled during the experiment. All measurement devices were calibrated by calibration
254 instruments by comparing their accuracy with declared in the technical documentation in order
255 to exclude the above error. Connection between measurement devices and controllers was
256 provided with a maximum error of processing signals within 1.5%.

257 Creation of graphical dependences was carried out by differential methods of mathematical
258 analysis and integral calculus. Reliability of the obtained experimental results is due to
259 application of time-tested methods in practice.

260 2.3 Materials

261 Melt of ammonium nitrate and urea was used. Manufacturer of ammonium nitrate
262 (agrotechnical chemical) - PSC "Azot", Ukraine. Main parameters of ammonium nitrate –

263 according to [29].

264

265

3. RESULTS AND DISCUSSION

266 The model of the jet decay is based on the solution of Navier-Stokes equations (11) - (12) and

267 the flow continuity equation (13) in cylindrical coordinates [9], with the following

268 simplifications:

269 - flow is axially symmetric;

270 - cross-section of the jet is circular, there is only jet restriction and extension (the tangential

271 component of jet velocity $u_{\theta}=0$).

$$272 \quad u_r \frac{\partial u_r}{\partial r} = -\frac{1}{\rho} \cdot \frac{\partial p}{\partial r} + \nu \cdot \left[\frac{\partial^2 u_r}{\partial z^2} + \frac{\partial}{\partial r} \cdot \left(\frac{\partial}{\partial r} r \cdot u_r \right) \right], \quad (11)$$

$$273 \quad u_z \frac{\partial u_z}{\partial z} = -\frac{1}{\rho} \cdot \frac{\partial p}{\partial z} + \nu \cdot \left[\frac{\partial^2 u_z}{\partial z^2} + \frac{1}{r} \cdot \frac{\partial}{\partial r} \cdot \left(r \cdot \frac{\partial u_z}{\partial r} \right) \right], \quad (12)$$

$$274 \quad \frac{\partial u_z}{\partial z} + \frac{1}{r} \cdot \frac{\partial}{\partial r} \cdot r \cdot u_r = 0. \quad (13)$$

275 By assuming that the axial velocity component at the time of leaving the hole varies

276 parabolically with the radial coordinate:

$$277 \quad u_z = A_1 \cdot r^2 + A_2 \cdot r + A_3, \quad (14)$$

278 and transforming the equation (13), we obtain the value of the radial component of the jet

279 velocity:

$$280 \quad u_r = \frac{-\frac{1}{2} \cdot A_1 \cdot r^4 \cdot z + F_1 \cdot z}{r} \quad (15)$$

281 where $F_1(z)$ is polynomial function.

282 Given the fact that the pressure change in a jet in the radial direction is insignificant compared
 283 to the axial component, and by substituting (14) into (12) we get:

$$284 \quad 2 \cdot A_1 \cdot r^2 \cdot z^2 + A_2 \cdot r + A_3 \quad A_1 \cdot r^2 \cdot z = \frac{1}{\rho} \cdot \frac{dp}{dz} + v \cdot \left(2 \cdot A_1 \cdot r^2 + \frac{4 \cdot A_1 \cdot r \cdot z^2 + A_2}{r} \right). \quad (16)$$

285 By solving the equation (16) for dp/dz and by integration the expression for pressure change
 286 along the jet axis is obtained:

$$287 \quad p(z) = -\frac{1}{r} \cdot \left(\rho \cdot \left(\frac{1}{2} \cdot A_1^2 \cdot r^5 \cdot z^4 + A_1 \cdot r^4 \cdot z^2 \cdot A_2 + A_1 \cdot r^3 \cdot z^2 \cdot A_3 - 2 \cdot v \cdot A_1 \cdot r^3 \cdot z - \frac{4}{3} \cdot v \cdot A_1 \cdot r \cdot z^3 - v \cdot A_2 \cdot z \right) \right) + C_1 \quad (17)$$

288 By setting the origin of the coordinate system at the hole exit ($z=0$) and by introducing the
 289 assumption that the liquid outflow occurs at a constant pressure ($p = \text{const}$), then according to
 290 (17) it is obtained that $C_1 = p_1$.

291 After insertion of this constant we get:

$$292 \quad p(z) = -\frac{1}{r} \cdot \left(\rho \cdot \left(\frac{1}{2} \cdot A_1^2 \cdot r^5 \cdot z^4 + A_1 \cdot r^4 \cdot z^2 \cdot A_2 + A_1 \cdot r^3 \cdot z^2 \cdot A_3 - 2 \cdot v \cdot A_1 \cdot r^3 \cdot z - \frac{4}{3} \cdot v \cdot A_1 \cdot r \cdot z^3 - v \cdot A_2 \cdot z \right) \right) + p_1 \quad (18)$$

293 By inserting (18) into (11):

$$294 \quad \frac{\left(-\frac{1}{2} \cdot A_1 \cdot r^4 \cdot z + F_1(z) \right) \left(-2 \cdot A_1 \cdot r^2 \cdot z - \frac{-\frac{1}{2} \cdot A_1 \cdot r^4 \cdot z + F_1(z)}{r^2} \right)}{r} = -\frac{1}{\rho} \cdot \left(\frac{1}{r^2} \cdot \left(\rho \cdot \left(\frac{1}{2} \cdot A_1^2 \cdot r^5 \cdot z^4 + A_1 \cdot r^4 \cdot z^2 \cdot A_2 + \right. \right. \right.$$

$$295 \quad \left. \left. + A_1 \cdot r^3 \cdot z^2 \cdot A_3 - 2 \cdot v \cdot A_1 \cdot r^3 \cdot z - \frac{4}{3} \cdot v \cdot A_1 \cdot r \cdot z^3 - v \cdot A_2 \cdot z \right) \right) - \frac{1}{r} \cdot \left(\rho \cdot \left(\frac{5}{2} \cdot r^4 \cdot A_1^2 \cdot z^4 + 4 \cdot A_1 \cdot r^3 \cdot z^2 \cdot A_2 + \right. \right.$$

$$296 \quad \left. \left. + 3 \cdot A_1 \cdot r^2 \cdot z^2 \cdot A_3 - 6 \cdot v \cdot A_1 \cdot r^2 \cdot z - \frac{4}{3} \cdot v \cdot A_1 \cdot z^3 \right) \right) + v \cdot \left(\frac{1}{r} \cdot \frac{d^2 F_1(z)}{dz^2} - 4 A_1 \cdot r \cdot z \right) \quad (19)$$

297 we obtain the differential equation of total derivatives in respect to the function $F_1(z)$. Based on
 298 the fact that the derivative du_r/dz is equal to:

$$299 \quad \frac{du_r}{dz} = \frac{-\frac{1}{2} \cdot A_1 \cdot r^4 \cdot z + \frac{dF_1}{dz} \cdot z}{r}, \quad (20)$$

300 and the radial velocity component of the jet at $z=0$ becomes $u_r=0$, we obtain:

$$301 \quad \frac{1}{2} A_1 \cdot r^4 \cdot z = \frac{dF_1}{dz} \cdot z. \quad (21)$$

302 By using the boundary conditions $F_1(z=0)=0$ and $dF_1/dz (z=0)=0$, and put them into the equation

303 (14) we obtain the value of the function F_1 as a polynomial:

$$304 \quad F_1(z) = \frac{1}{6} \cdot \frac{(-A_2 + 8 \cdot A_1 \cdot r^3) \cdot z^3}{r} + \frac{1}{48} \cdot \frac{A_1 \cdot r^2 \cdot (3 \cdot A_1 \cdot r^4 - 12 \cdot A_2 \cdot r - 8 \cdot A_3) \cdot z^4}{v}. \quad (22)$$

305 Substituting the relation (22) in the equation (15) leads to:

$$306 \quad u_r = \frac{1}{48} \cdot \frac{z \cdot (-24 \cdot A_1 \cdot r^5 \cdot v - 8 \cdot v \cdot z^2 \cdot A_2 + 64 \cdot v \cdot z^2 \cdot A_1 \cdot r^3 + 3 \cdot A_1^2 \cdot r^7 \cdot z^3 - 12 \cdot A_1 \cdot r^4 \cdot z^3 \cdot A_2 - 8 \cdot A_1 \cdot r^3 \cdot z^3 \cdot A_3)}{v \cdot r^2}. \quad (23)$$

307 The coefficient A_2 can be found by assuming that on the jet surface $r=r_s$ the pressure p is equal

308 to the pressure of the surrounding environment p_0 . This boundary condition can be written as:

$$309 \quad p_0 = -\frac{1}{r_s} \cdot \left(\rho \cdot \left(\frac{1}{2} \cdot A_1^2 \cdot r_s^5 \cdot z^4 + A_1 \cdot r_s^4 \cdot z^2 \cdot A_2 + A_1 \cdot r_s^3 \cdot z^2 \cdot A_3 - 2 \cdot v \cdot A_1 \cdot r_s^3 - \frac{4}{3} \cdot v \cdot A_1 \cdot r_s \cdot z^3 - v \cdot A_2 \cdot z \right) \right) + p_1 \quad (24)$$

310 Thus, the coefficient A_2 is now calculated as:

$$311 \quad A_2 = -\frac{1}{6} \cdot \frac{(r_s \cdot (3 \cdot z^4 \cdot A_1^2 \cdot \rho \cdot r_s^4 + 6 \cdot z^2 \cdot A_1 \cdot \rho \cdot r_s^2 \cdot A_3 - 12 \cdot z \cdot A_1 \cdot \rho \cdot v \cdot r_s^2 - 8 \cdot \rho \cdot v \cdot A_1 \cdot z^3 - 6 \cdot p_1 + 6 \cdot p_0))}{\rho \cdot z \cdot (A_1 \cdot r_s^4 \cdot z - v)}. \quad (25)$$

312 The coefficient A_3 can be defined by assuming that that if $r=0$, $u_r=0$:

$$313 \quad A_3 = -\frac{1}{6} \cdot \frac{3 \cdot z^4 \cdot A_1^2 \cdot \rho \cdot r_s^4 + 6 \cdot p_0 - 12 \cdot z \cdot A_1 \cdot \rho \cdot v \cdot r_s^2 - 8 \cdot \rho \cdot v \cdot A_1 \cdot z^3 - 6 \cdot p_1}{z^2 \cdot r_s^2 \cdot \rho \cdot A_1}. \quad (26)$$

314 Accordingly,

$$315 \quad u_z = A_1 \cdot r^2 \cdot z^2 - \frac{1}{6} \cdot \frac{3 \cdot z^4 \cdot A_1^2 \cdot \rho \cdot r_s^4 + 6 \cdot p_0 - 12 \cdot z \cdot A_1 \cdot \rho \cdot v \cdot r_s^2 - 8 \cdot \rho \cdot v \cdot A_1 \cdot z^3 - 6 \cdot p_1}{z^2 \cdot r_s^2 \cdot \rho \cdot A_1}. \quad (27)$$

316 The coefficient A_1 is determined by assuming that at a point close to the origin of the
 317 coordinate system $z = z_0$, the exhaust velocity has not yet changed its value and is equal to the
 318 flow velocity jet in the hole $u_z = u_{z_0}$ that is:

$$319 \quad u_{z_0} = \frac{1}{6} \cdot \frac{6 \cdot A_1^2 \cdot r^2 \cdot z_0^4 \cdot r_s^2 - 3 \cdot z_0^4 \cdot A_1^2 \cdot \rho \cdot r_s^4 - 6 \cdot p_0 - 12 \cdot z_0 \cdot A_1 \cdot \rho \cdot v \cdot r_s^2 + 8 \cdot \rho \cdot v \cdot A_1 \cdot z_0^3 + 6 \cdot p_1}{z_0^2 \cdot r_s^2 \cdot \rho \cdot A_1}. \quad (28)$$

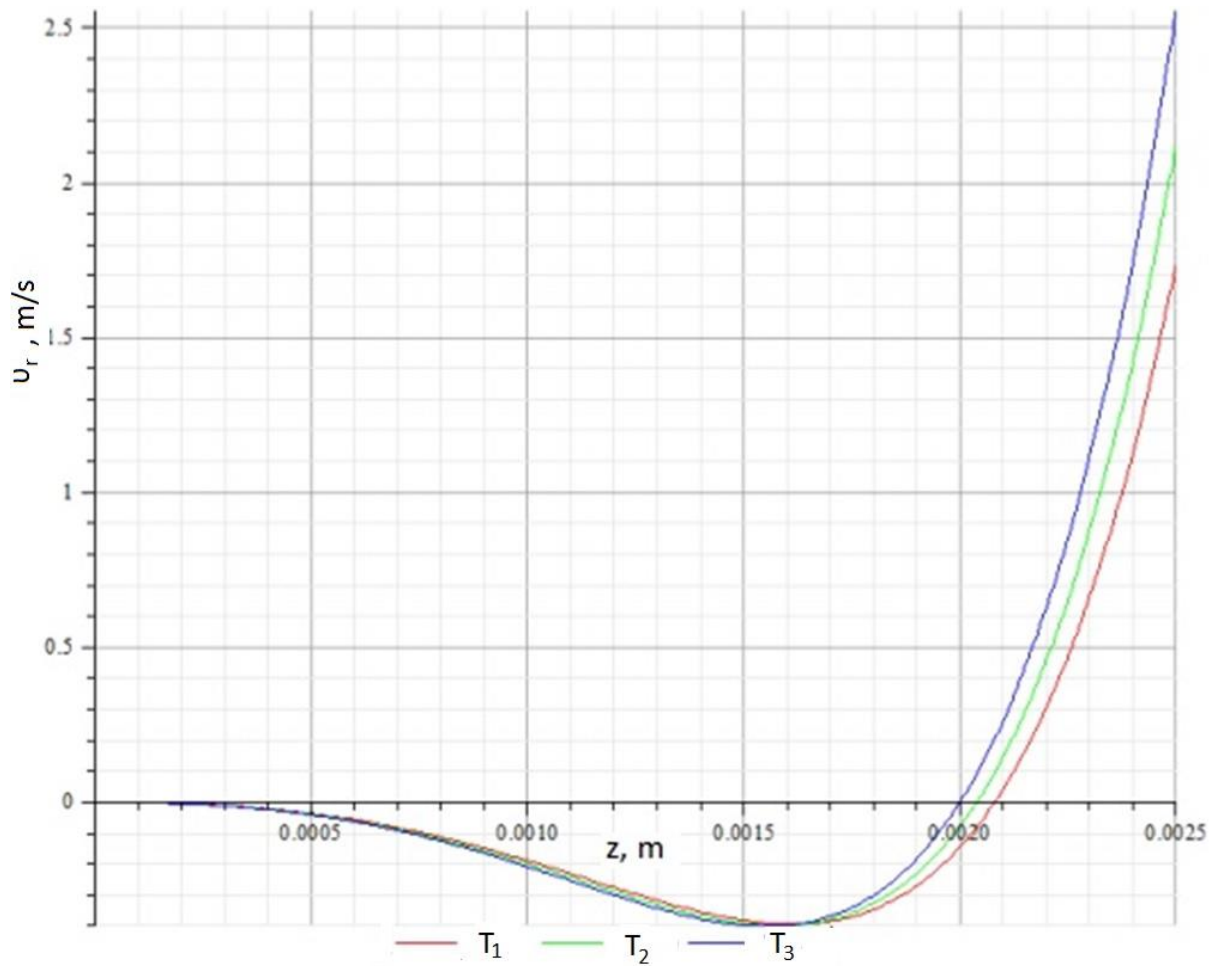
320 When we solve the resulting equation (28) for the coefficient A_1 , we obtain:

$$321 \quad A_1 = \frac{1}{3} \cdot \frac{1}{z_0^3 \cdot r_s^2 \cdot \rho \cdot (2 \cdot r^2 - r_s^2)} (-4 \cdot v \cdot \rho \cdot z_0^2 + 3 \cdot u_{z_0} \cdot r_s^2 \cdot \rho \cdot z_0 - 6 \cdot \rho \cdot v \cdot r_s^2 + (16 \cdot v^2 \cdot \rho^2 \cdot z_0^4 -$$

$$322 \quad -24 \cdot v \cdot \rho^2 \cdot z_0^3 \cdot u_{z_0} \cdot r_s^2 + 48 \cdot v^2 \cdot \rho^2 \cdot z_0^2 \cdot r_s^2 + 9 \cdot u_{z_0}^2 \cdot r_s^4 \cdot \rho^2 \cdot z_0^2 - 36 \cdot u_{z_0} \cdot r_s^4 \cdot \rho^2 \cdot z_0 \cdot v + 36 \cdot \rho^2 \cdot v^2 \cdot r_s^4 +$$

$$323 \quad 36 \cdot z_0^2 \cdot r^2 \cdot r_s^2 \cdot \rho \cdot p_0 - 36 \cdot z_0^2 \cdot r^2 \cdot r_s^2 \cdot \rho \cdot p_0 - 36 \cdot z_0^2 \cdot r^2 \cdot r_s^2 \cdot \rho \cdot p_1 - 18 \cdot z_0^2 \cdot r_s^4 \cdot \rho \cdot p_0 + 18 \cdot z_0^2 \cdot r_s^4 \cdot \rho \cdot p_1)^{1/2}) \quad (29)$$

324 The presented mathematical model allows calculating radial and axial components of the
 325 velocity jet outflow, as well as to establish the influence of physical and chemical properties of
 326 the liquid and the hole diameter on the jet length and velocity along the axis to its disintegration
 327 into separate drops (Figs 2, 3).



328

329 **Fig. 2. Dependence of the radial component of the jet velocity of the ammonium nitrate melt**

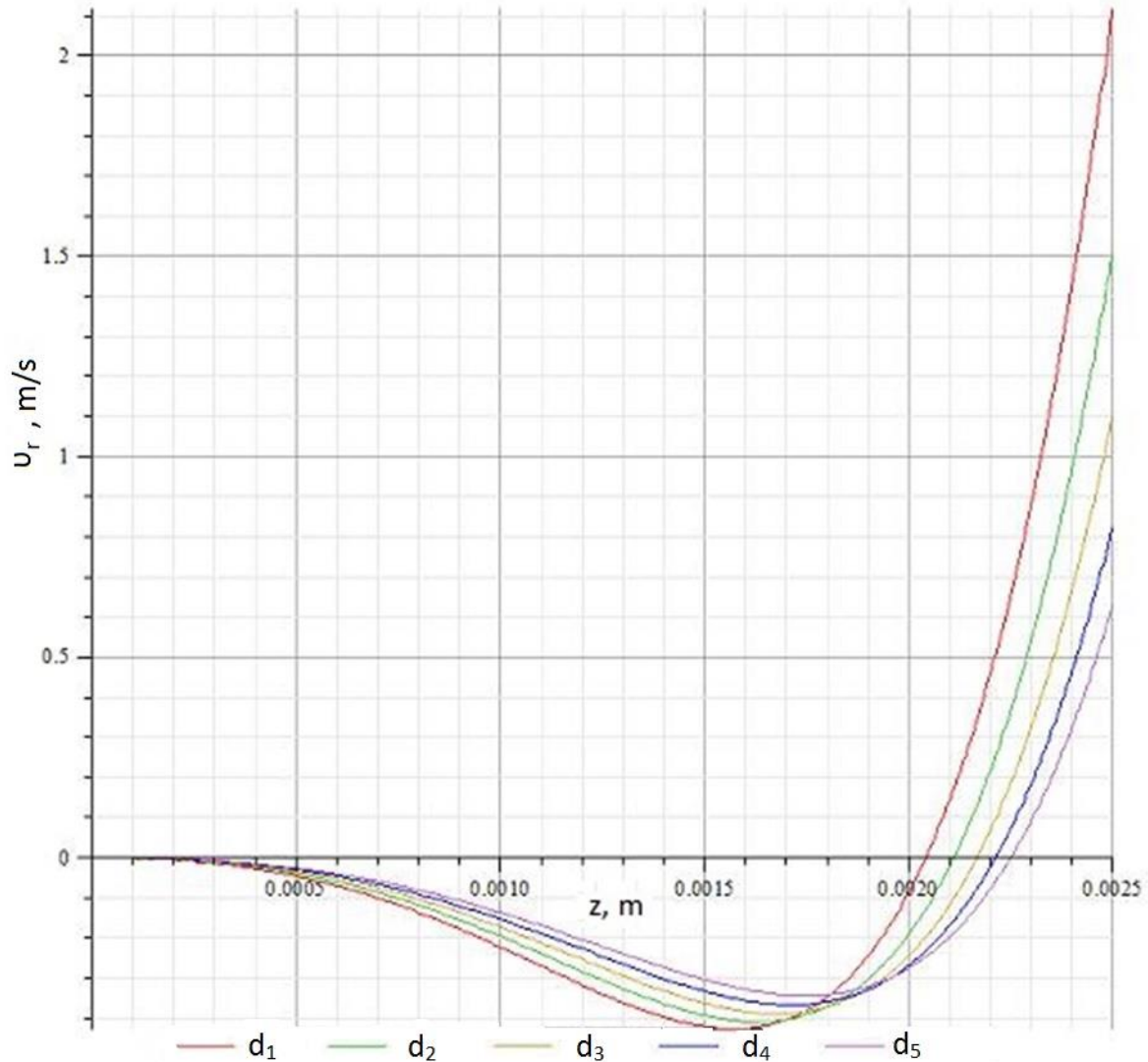
330 **on the axial distance, z, from the hole diameter of 1.3 mm at different temperatures of the**

331 **melt at $T_1 = 175^\circ\text{C}$, $T_2 = 180^\circ\text{C}$, $T_3 = 185^\circ\text{C}$ and the vibration frequency of 340 Hz (viscosities**

332 **were 5.36, 5.03, 4.74 mPa·s, densities were 1434, 1431, 1428 kg/m³ respectively). Granulator**

333 **basket rotation velocity was $n = 60$ rpm and a load of 37 t/h.**

334



335
 336 **Fig. 3. Dependence of the radial component of the jet velocity of the ammonium nitrate melt**
 337 **on the axial distance, z , from the holes of different diameters: $d_1=1.0$ mm, $d_2=1.1$ mm, $d_3=1.2$**
 338 **mm, $d_4=1.3$ mm, $d_5=1.4$ mm at the temperature of 185°C (viscosity was 4.74 mPa·s, density**
 339 **was 1428 kg/m³) and the vibration frequency of 340 Hz. Granulator basket rotation velocity**
 340 **was $n = 60$ rpm and a load of 37 t/h.**

341 The radial component of the velocity scarcely appears at the short distance from the hole.
 342 When the distance increases, there are radial flows in the jet, which cause its breaking-up into
 343 drops. It is indicated by the significant increase of the radial component. An increase in the

344 temperature of the melt and the diameter of the perforated shell hole leads to the reduction of
345 the distance from the hole, at which the radial component becomes critical, at which the jet is
346 broken up. The negative velocity indicates the breakoff of flow (detachment of the jet with the
347 formation of the vortex flows), which disappears with an increase of parameter z .

348 The smaller the distance from the outflow hole during jet breaking-up, the smaller the length of
349 the jet portion, which forms the volume of drop during jet breaking-up. This hypothesis
350 coincides with the results of other scientists' studies [30].

351 For granulator basket rotation velocity $n = 60$ rpm and a load of 37 t/h optimal diameter of the
352 hole is $d=1.2$ mm, the melt temperature is 185°C .

353 An example of comparison of theoretical calculations and experimental results of velocity radial
354 component measurement was shown in Table 1.

355

356

357

358

359

360

361

362

363

364

365

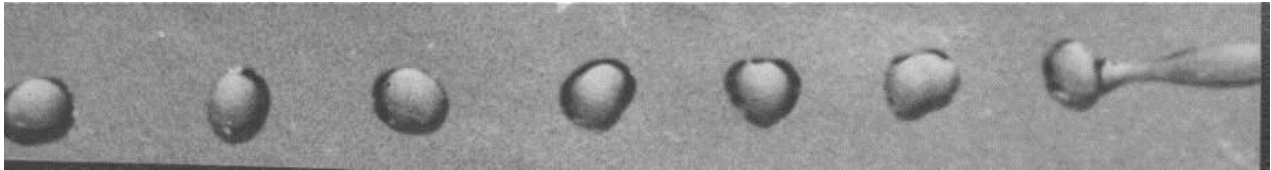
366 Table 1. An example of comparison of theoretical calculations and experimental results of u_r
 367 measurement (hole diameter was 1.3 mm, temperatures of the melt was 175°C (viscosity was
 368 5.36 mPa·s, density was 1434 kg/m³), vibration frequency was 340 Hz, granulator basket
 369 rotation velocity was $n = 60$ rpm and a load was 37 t/h)

z=0 m			z=0.0005 m		
$u_{r.theor}, m/s$	No of measurement	$u_{r.exp}, m/s$	$u_{r.theor}, m/s$	No of measurement	$u_{r.theor}, m/s$
0	1	0	-0.05	1	-0.04
0	2	-0.003	-0.05	2	-0.02
0	3	0.002	-0.05	3	-0.08
0	4	0	-0.05	4	-0.07
0	5	0.004	-0.05	5	-0.09
0	6	-0.005	-0.05	6	-0.04
z=0.001 m			z=0.0015 m		
$u_{r.theor}, m/s$	No of measurement	$u_{r.exp}, m/s$	$u_{r.theor}, m/s$	No of measurement	$u_{r.theor}, m/s$
-0.2	1	-0,21	-0,4	1	-0,4
-0.2	2	-0,19	-0,4	2	-0,42
-0.2	3	-0,19	-0,4	3	-0,39
-0.2	4	-0,19	-0,4	4	-0,38
-0.2	5	-0,18	-0,4	5	-0,4
-0.2	6	-0,2	-0,4	6	-0,41
z=0.002 m			z=0.0025 m		
$u_{r.theor}, m/s$	No of measurement	$u_{r.exp}, m/s$	$u_{r.theor}, m/s$	No of measurement	$u_{r.theor}, m/s$
0	1	-0,01	2.5	1	2,44
0	2	0,01	2.5	2	2,53
0	3	0,02	2.5	3	2,51
0	4	0	2.5	4	2,41
0	5	-0,03	2.5	5	2,56
0	6	0	2.5	6	2,6

370

371 Basket tests of the granulator (shown in Fig. 1) confirmed the theoretical research and provided
372 a basis for modernization of the equipment construction. During the tests, a stable jet breakup
373 into drops at a distance of 2-5 mm from the wall of the perforated shell was obtained (Figs 4, 5).

374



375

376

a



377

378

b

379 **Fig. 4. Jet disintegration into drops after the outflow from the perforated shell: a) ammonium**
380 **nitrate drops, vibration frequency of 200 Hz; b) ammonium nitrate drops, vibration frequency**
381 **of 340 Hz. Diameter of hole was 1.1 at the temperature of 185°C (viscosity was 4.74 mPa·s,**
382 **density was 1428 kg/m³). Granulator basket rotation velocity was n = 60 rpm and a load of 37**
383 **t/h.**

384



385

386 **Fig. 5. Steady jet disintegration into drops after the outflow from the perforated shell:**

387 **ammonium nitrate drops, vibration frequency of 340 Hz. Diameter of hole was 1.1 at the**

388 **temperature of 185°C (viscosity was 4.74 mPa·s, density was 1428 kg/m³). Granulator basket**

389 **rotation velocity was $n = 60$ rpm and a load of 37 t/h.**

390 The developed mathematical model was extended with the theoretical description of the melt

391 dispersion process from rotating perforated shells, which allowed us to improve the granulator

392 design to stabilize hydrodynamic parameters of the melt movement within it. By applying of a

393 weighted vortex layer in combination with the vibrating material liquid spray and rotation of

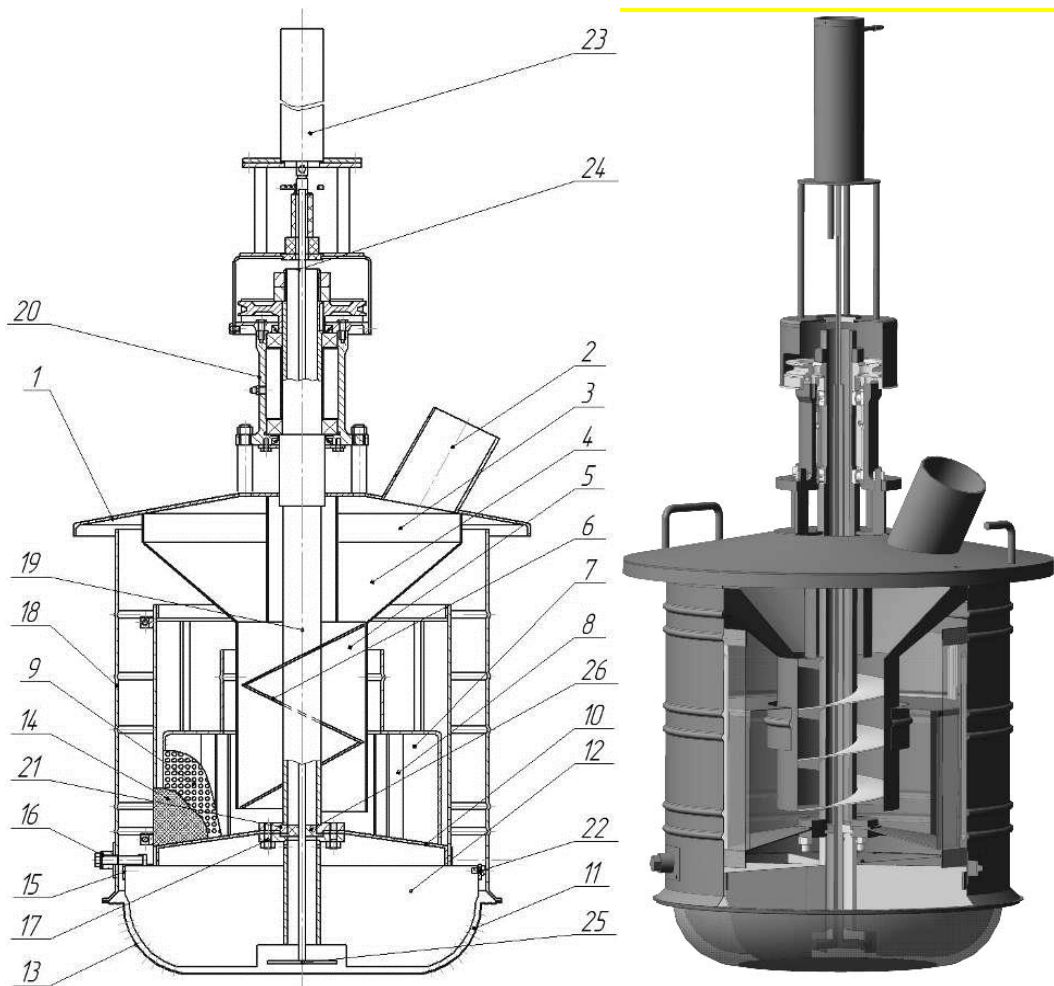
394 liquid jets by their decay will further improve the quality of the granulated product.

395 **Scheme of the modernized granulator is shown in Fig. 6, and layout solutions for granulator**

396 **installation in the granulation tower in Fig. 7. Similarity of respective particles movements and**

397 their trajectories in industrial design and in experimental models as maintained.

398 Installation of a guiding element in the form of an auger into the granulator, when the melt
 399 contacts with the shoulder blade, increases the melt total pressure by transforming the screw
 400 mechanical energy into the melt kinetic energy and then turning it into the internal energy. The
 401 possibility of screw rotation provides the option for increasing the pressure before the outflow
 402 holes.



403
 404 **Fig. 6. Rotating vibration granulator of solutions (melts): 1 - housing; 2 - pipe for introducing**
 405 **the solution (melt); 3 - ring collector; 4 - reverse cone; 5 - annular channel; 6 - auger; 7 -**
 406 **distributor of the solution (melt); 8 - directing blades; 9 - perforated cylinder; 10 - directing**
 407 **cone for the solution (melt); 11 - perforated bottom (basket); 12 - pressure blades; 13 - hole;**

408 **14 - mesh for the final melt filtration; 15 - ring; 16 - bolts; 17 - pins; 18 - cylindrical chamber;**
409 **19 - hollow shaft; 20 - bearing assembly; 21 - flange connection; 22 - bulge for centering the**
410 **cylindrical chamber; 23 - vibration device; 24 - rod; 25 - disc radiant; 26 - hub.**

411



412

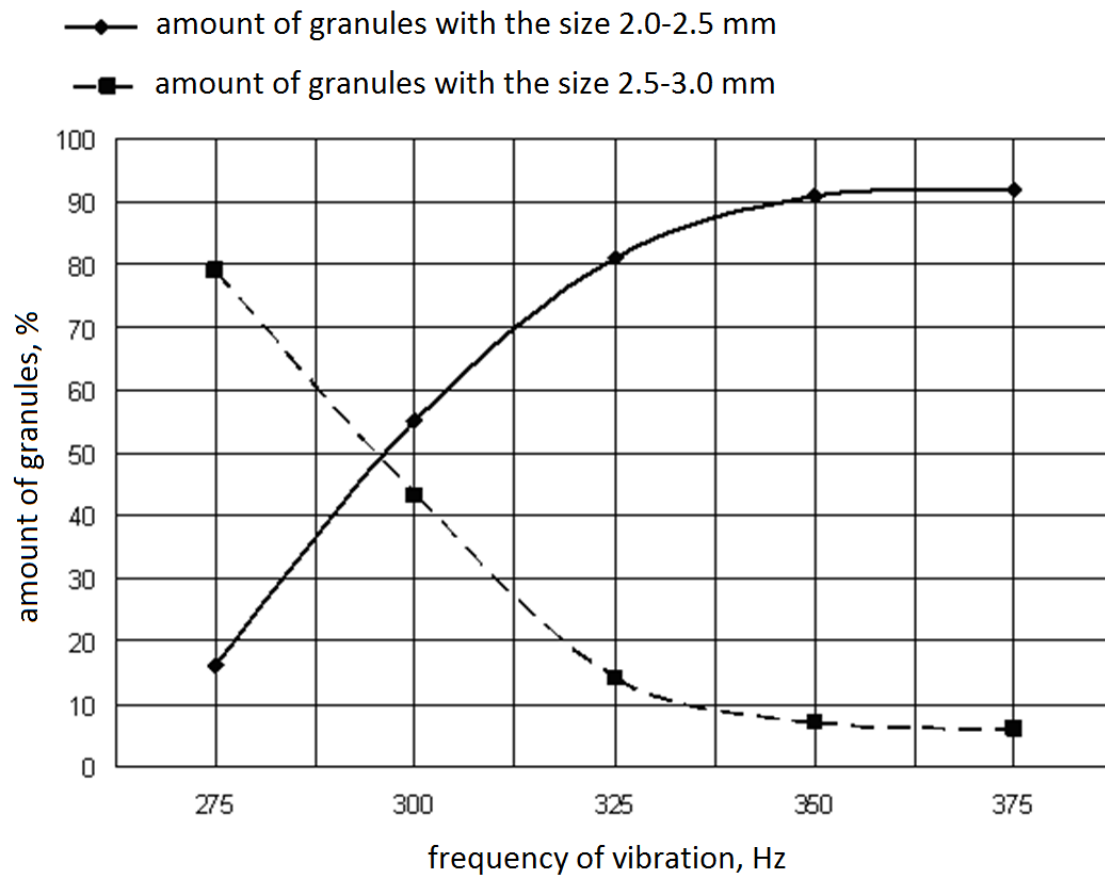
413 **Fig. 7. The layout solutions for granulator installation in the granulation tower**

414 Pilot testing of the modified granulator of the total capacity of **37 t/h** in production of
415 ammonium nitrate for different climatic conditions (humid and hot climate, temperate
416 continental type) showed a higher yield of marketable fractions and reduction of dust content in
417 flue gases.

418 High level of monodispersity of granules is achieved by improving the fusion hydrodynamics in
419 the granulator, improving the process of applying vibration to the jets of substance that leak out
420 from the basket perforated bottom.

421 Also the modified granulator significantly reduced the granulated product dust level in the air
422 coming out of the tower. Axial flow fans capture from 16 to 38 mg/m³ of dust so that the
423 granulator enables the company to reduce the considerable funds necessary for purchasing
424 expensive new equipment to clean the air coming out of the tower.

425 The basic granulator test results are shown in Figs 8-9.

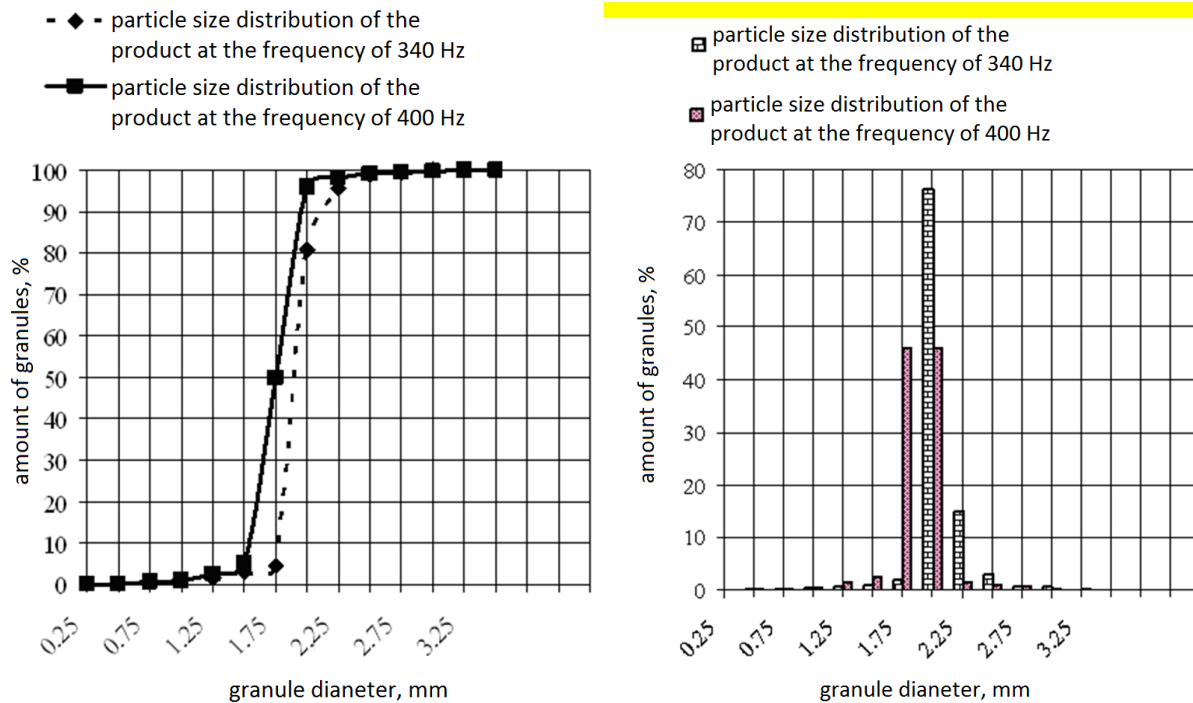


426

427 **Fig. 8. Mass fractions of ammonium nitrate granules with sizes 2.0 – 2.5 mm and 2.5 - 3.0 mm**
428 **as functions of the vibration frequency at the granulator basket rotation velocity of $n = 60$**
429 **rpm and a load of 37 t/h and the hole diameter of 1.2 mm**

430

431



432

433

a

b

434

Fig. 9. The integral particle size distribution of ammonium nitrate granules at vibration

435

frequencies of 340 and 400 Hz and the granulator basket rotation velocity of $n = 60$ rpm, load

436

of 37 t/h and the hole diameter of 1.2 mm: a) line graph b) bar chart

437 Analysis of Fig. 6-8 provides determination of an optimal (operating) vibration frequency

438 (frequency range), at which the maximal degree of monodispersity of the drops is achieved.

439 Therefore, the melt jet disintegrates evenly and without formation of drop satellites.

440 The monodispersion process introduces a fundamental improvement in the fertilizer production

441 technology. The use of uniform (monodisperse) granules, for example in agriculture, provides an

442 even distribution of the fertilizer on the fertilized area resulting in the additional yield up to 10%

443 [10-12].

444 Vibrating granulators provide production of strong monodisperse granules with a smooth glossy

445 surface (the monodispersity degree is up to 99 %). It opens the possibility to intensify the

446 granulation process and essentially improves the agrotechnical value of fertilizers.

447 Table 2 shows a comparative analysis of the granulometric composition of the final product in
448 different types of granulators.

449 Table 2. Comparison of rotating vibration granulators with world analogues of the granulation
450 equipment in granulation towers

Granulometric composition, %	Centrifugal granulator of firm "Kreber" (Netherlands) [31]	Acoustics granulator designed by Research Institute at the Chemical plant (Russia) [32]	Rotating vibration granulators (this work)
- 1-4 mm	97-99	98-99	more than 99
- 2-4 mm	83-92	85-95	90-97
- 2-3 mm	75-90	80-90	more than 90
- 2.0-2.5 mm	40-50	45-65	more than 80
- less than 1 mm	0.8-2,5	0.8-1.5	0.1-0.8

451
452 The improved granulator has the following advantages over other granulator types (on the basis
453 of literature review, e.g. [33-37]):

454 - high safety in operation;

455 - production of more competitive uniform granules;

456 - avoidance of the product's sticking in towers;

457 - decrease of dust arising;

458 - increase of the agro-technical value of fertilizers.

459 The vibrating granulators have a reliable vibration system, which provides a stable imposition of
460 oscillations on the fluid jets, flowing out of perforated shell holes, regardless the changes in the
461 load on the melt disperser. This vibration system provides measurements of the level of melt in
462 the granulator and thereby, to control the clogging degree and the melt outflow velocity from
463 the holes of the perforated shell.

464 The vibrating granulator (fig. 6) with an electromagnetic vibration system (vibration frequency
465 of 340 Hz) provided production of a product with the following granulometric composition as
466 mass fractions: 0.02-0.2% of granules < 1.0 mm and over 96% of granules 2.0 - 4.0 mm in size.
467 Also, for the fraction of granules in the size range 2.0 - 2.5 mm was not lower than 88% with the
468 main size in the range 2.1-2.5 mm. When the vibration frequency was changed to 400 Hz , the
469 granulator provided production of the product with the main fraction (over 65 %) of granules of
470 2.5 - 3.0 mm simultaneously increasing the hardness of the main fraction granules (hardness
471 value was confirmed in [12]).

472 Similar results of granulometric compositions of products were obtained on vibrating
473 granulators with electromagnetic vibration systems in the ammonium nitrate production under
474 tropical conditions in Cuba and urea with foaming additives of hydrohumates [12]. During the
475 industrial operation of this device the product (urea) with the following granulometric
476 composition in mass fractions was stably obtained during one month: 0.1 - 0.3 % of granules <
477 1.0 mm, 99.7 - 99.9 % of granules in the size range 1.0-4.0 mm where granules in the size range
478 2.0 - 4.0 mm comprised 96.5-98.9% while granules of a size larger than 4.0 mm were absent.

479

4. CONCLUSION

480 Consideration of hydrodynamic parameters of the liquid jet flowing out of holes of a perforated
481 membrane allowed us to affect parameters of the process of jet decay into drops, drop size and
482 dispersity and consequently to improve the construction of a nitrogen fertilizers melt
483 granulator.

484 **Main results:**

485 - the mathematical model to calculate hydrodynamic properties of the melt jet expiration
486 process from a perforated shell is formed;

487 - the influence of the holes diameter and melt properties on the radial velocity field is shown;

488 - the optimal conditions for prilling in a vibrating granulator for a given capacity of 37 t / h are
489 defined: the rotation velocity of the basket, the diameter of the holes in the perforated shell,
490 the melt temperature, the frequency range of the actuator's oscillation;

491 - the modernized construction of the vibrating granulator is given

492 - results regarding industrial tests of the modernized vibrating granulator are presented, the
493 technological features of the work of which complied with the optimal conditions of the prilling.

494 *Acknowledgements:* The authors thank researchers at the Processes and Equipment of Chemical
495 and Petroleum Refinery Department, Sumy State University and the Department of Numerical
496 Methods and Computational Modeling, Alexander Dubcek University of Trencin for their
497 valuable comments during the article preparation.

498 This research work had been supported by the Cultural and Educational Grant Agency of the
499 Slovak Republic (KEGA), project No. KEGA 002TnUAD-4/2019 and by the Ministry of Science and
500 Education of Ukraine under the project «Small-scale energy-saving modules with the use of

501 multifunctional devices with intensive hydrodynamics for the production, modification and
502 encapsulation of granules», project No. 0119U100834.

503 **Symbols**

504 A_1, A_2, A_3 – coefficients of parabolic equation;

505 C_1 – differential equation solution constant;

506 d_{dr} - diameter of drop, m;

507 $d_{dr}^{max}, d_{dr}^{min}$ – bigger and smaller diameter of drops, m (mm);

508 Δd_{dr}^{ab} – absolute difference of drop diameters, m;

509 Δd_{dr}^{rel} – relative deviation of drop diameters;

510 $F_1(z)$ – polynomial function;

511 f_1, f_2 – upper and lower limits of frequency, 1/s;

512 f_{avi} – average frequency of vibration, which provides monodisperse jets decay, 1/s;

513 g – acceleration of gravity, m/s^2 ;

514 G_s – melt flowrate, m^3/s ;

515 G_t – the measured volume of the melt, m^3 ;

516 H – liquid column height (head), m;

517 n – number of measurements; granulator basket rotation velocity, rpm;

518 p – the outflow jet pressure, Pa;

519 p_0 – pressure of the surrounding environment, Pa;

520 r – radius of the jet, m;

521 t – the Student's criterion;

522 V – velocity of the liquid leaking from the granulator holes, m/s;

523 \bar{x} – arithmetic mean value;

524 x – single parameter value;

525 z_0 – initial axial distance, holes, m;

526 z – axial distance, holes, m;

527 Δ – maximum possible error of a single measurement, %;

528 ϵ – bilateral confidence interval of the arithmetic mean value;

529 $\lambda_{\max}, \lambda_{\min}$ – maximum and minimum lengths of the wave, m;

530 ρ – liquid density, kg/m^3 ;

531 σ – root-mean-square deviation;

532 τ – the experimental time of melt outflow through the granulator hole, s.

533 u_θ, u_r, u_z – tangential, radial and axial components of the jet velocity respectively, m/s;

534 u_{z_0} – initial axial component of the jet velocity respectively, m/s;

535 ϕ – discharge coefficient.

536

537

538 REFERENCES

539 [1] Feng L, Liu M, Wang J, Sun J, Wang J, Mao Y. Study on the flow instability of a
540 spray granulation tower. *Sep Purif Technol.* 2016; 169:210–222.

541
542 [2] Artyukhov AE, Obodiak VK, Boiko, PG, Rossi PC. Computer modeling of hydrodynamic
543 and heat-mass transfer processes in the vortex type granulation devices. *CEUR*
544 *Workshop Proceedings.* 2017; 1844: 33-47.

545
546 [3] Artyukhov AE, Sklabinskyi VI. Hydrodynamics of gas flow in small-sized vortex
547 granulators in the production of nitrogen fertilizers. *Chem Chem Technol.* 2015; 9(3):
548 337-342.

549
550 [4] Urea Casale S.A. [E-text type]. Location of document: <http://www.casale.ch/>.

551
552 [5] Kahl Group [E-text type]. Location of document: <http://www.amandus-kahl-group.de>.

553
554 [6] Stamicarbon [E-text type]. Location of document: <http://www.stamicarbon.ru>.

555
556 [7] Toyo Engineering Corporation [E-text type]. Location of document: [http://www.toyo-](http://www.toyo-eng.com)
557 [eng.com](http://www.toyo-eng.com).

558

- 559 [8] Glatt Innovative Technologies for Granules and Pellets [[E-text type]. Location of
560 document: <http://www.glatt.com>.
561
- 562 [9] Artyukhov AE, Sklabinskyi VI. Theoretical analysis of granules movement
563 hydrodynamics in the vortex granulators of ammonium nitrate and carbamide
564 production. *Chem Chem Technol.* 2015; 9(2): 175–180.
565
- 566 [10] Sklabinskyi VI, Skydanenko MS., Kononenko NP. Technical audit of melt granulation
567 knots in the production of mineral fertilizers using tower method. *Tech Aud Prod Res.*
568 2014; 3(2): 16–23.
569
- 570 [11] Norsk Hydro [E-text type]. Location of document: <https://www.hydro.com/en>
571
- 572 [12] Sklabinskyi VI, Artyukhov AE, Kononenko MP, Rossi PC. Quality improvement of
573 granular nitrogen fertilizer in the prilling plants. In *CLICAP 2015: Congreso*
574 *Latinoamericano de Ingeniería y Ciencias Aplicadas. Argentina, 2015, pp. 611-618.*
575
- 576 [13] Wu Y, Bao C, Zhou Y. An Innovated Tower-fluidized Bed Prilling Process. *Chin J Chem.*
577 *Eng.* 2007; 15: 424–428.
578
- 579 [14] Saleh SN, Ahmed SM, Al-mosuli D, Barghi S. Basic design methodology for a prilling
580 tower. *Can J Chem Eng.* 2015; 93: 1403–1409.

581

582 [15] Gezerman AO, Corbacioglu BD. New approach for obtaining uniform-sized granules by
583 prilling process. *Chem Eng Elixir Chem Eng*. 2011; 40: 5225–5228.

584

585 [16] White F. *Fluid Mechanics*. Kindle Edition; 2015.

586

587 [17] Cengel YA, Cimbala JM. *Fluid Mechanics*. Special India; 2016.

588

589 [18] Harris FE. *Mathematics for Physical Science and Engineering: Symbolic Computing*
590 *Applications in Maple and Mathematica*. Academic Press; 2014.

591

592 [19] Hannan Z. *wxMaxima for Calculus I*. Zachary Hannan; 2015.

593

594 [20] Hannan Z. *wxMaxima for Calculus II*. Zachary Hannan; 2015.

595

596 [21] Vibrating granulator. Technical and commercial offer [E-text type]. Location of
597 document: <http://pohnv.teset.sumdu.edu.ua/uk/research/know-how.html> (in Ukrainian)

598

599 [22] Barsky E. *Entropic Invariants of Two-Phase Flows*. Amsterdam: Elsevier; 2015.

600

601 [23] Artyukhov A, Sklabinskiy V., Ivaniia A. Electrical intelligent system for controlling the
602 formation of monodisperse droplets in granulation devices based on magnetostrictive

603 actuator. Proceedings of the International Conference on Modern Electrical and Energy
604 Systems (MEES 2017). 2017; 280-283.

605

606 [24] Holin BG . Centrifugal and vibratory granulators and liquid sprayers. Moscow:
607 Mashinostroenie, 1977. (in Russian)

608

609 [25] Schulz HE. *Hydrodynamics – Concepts and Experiments*. InTech; 2015.

610

611 [26] Sahoo P. Probability and mathematical statistics. University of Louisville; 2013.

612

613 [27] Shao J. Mathematical Statistics. Springer-Science+Business Media; 2003.

614

615 [28] Rice JA. Mathematical Statistics and Data Analysis. Duxbury: Thomson Brooks/Cole;
616 2010.

617

618 [29] Pradyot P. Handbook of Inorganic Chemicals. McGraw-Hill; 2002

619

620 [30] Afanasyev VN. About some features of droplet flows Thermophysics of high
621 temperatures.1998; 36(1): 94–101. (in Ukrainian)

622

623 [31] Kreber [E-text type]. Location of document: [https://www.kreber.nl/markets/prilling-](https://www.kreber.nl/markets/prilling-nitrates)
624 [nitrates](https://www.kreber.nl/markets/prilling-nitrates)

625 [32] Research Institute at the Chemical plant [E-text type]. Location of document:

626 <https://www.niichimmash.ru/>

627

628 [33] Bin L, Zhongping X, Huixun L, Carlessi L. Prilling tower and process, in particular for
629 producing urea WO No 2014/060951, 2014.

630

631 [34] Snyder DM, Rizzi E. Granulation apparatus. IN No 224039, 2008.

632

633 [35] Rizzi E. Granulation Process and Apparatus. 2010/0289165, 2010.

634

635 [36] Bugarova Z, Polak A, Batyka D, Papp J. Process of preparation of granulated ammonium
636 nitrate-sulphate fertilizer. EP No 1595860, 2010.

637

638

639 [37] Artyukhov AE, Sklabinskyi VI. Experimental and industrial implementation of porous
640 ammonium nitrate producing process in vortex granulators. *Nauk Visn Nats Hirn Univ.*
641 2013; 6: 42–48.

642

643

644

645

646